LA-UR-01-5095
Approved for public release;
distribution is unlimited.

Title: **LORENTZ FORCE DETUNING ANALYSIS OF THE SPALLATION NEUTRON SOURCE (SNS) ACCELERATING CAVITIES**

Author(s): R. Mitchell, K. Matsumoto, G. Ciovati, K. Davis, K. Macha, and R. Sundelin

Submitted to:

LORENTZ FORCE DETUNING ANALYSIS OF THE SPALLATION NEUTRON SOURCE (SNS) ACCELERATING CAVITIES *

R. Mitchell†, K. Matsumoto, Los Alamos National Lab, Los Alamos, NM 87545, USA
G. Ciovati, K. Davis, K. Macha, R. Sundelin, Jefferson Lab, Newport News, VA 23606, USA

Abstract

The Spallation Neutron Source (SNS) project incorporates a superconducting radio-frequency (SRF) accelerator for the final section of the pulsed mode linac. Cavities with geometrical β values of β=0.61 and β=0.81 are utilized in the SRF section, and are constructed out of thin-walled niobium with stiffener rings welded between the cells near the iris. The welded titanium helium vessel and tuner assembly restrains the cavity beam tubes. Cavities with β values less than one have relatively steep and flat side-walls making the cavities susceptible to Lorentz force detuning. In addition, the pulsed RF induces cyclic Lorentz pressures that mechanically excite the cavities, producing a dynamic Lorentz force detuning different from a continuous RF system. The amplitude of the dynamic detuning for a given cavity design is a function of the mechanical damping, stiffness of the tuner/helium vessel assembly, RF pulse profile, and the RF pulse rate. This paper presents analysis and testing results to date, and indicates areas where more investigation is required.

1 LORENTZ FORCE DETUNING

RF power produces radiation pressures that act on the cavity wall. The pressures are a function of the surface electric and magnetic fields as shown below [1].

$$P = \frac{1}{4}\left(\mu_0 H^2 - \varepsilon_0 E^2\right)$$

The pressures deform the cavity wall, tending to act outward near the equator and inward near the iris (see Fig. 1). The cavity cell deformations produce a frequency shift as described below.

$$\Delta f = K_L E_{acc}^2$$

For the SNS cavities, the magnitude of the Lorentz force detuning coefficient (K_L) must be less than 3 Hz/(MV/m)^2. Because the SNS accelerator pulses the RF power at 60 Hz, the Lorentz detuning varies as a function of time and can produce Lorentz force detuning coefficients significantly different from a continuous RF system.

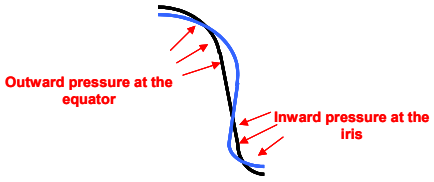

Figure 1: Lorentz pressures.

*Work supported by the Office of Basic Energy Science, Office of Science of the DOE, and ORNL.
†rrm@lanl.gov

2 SNS CAVITY ASSEMBLY

The medium β=.61 cavity is a thin wall (3.8mm) niobium structure that utilizes electron beam welding at the iris and equator (see Fig. 2). A stiffening ring is welded near the iris at an 80mm radius. The cavity is welded into a pure titanium helium vessel. One end of the cavity is welded directly to the helium vessel while the opposing end is attached to the helium vessel by the stainless steel tuner. The medium β cavities are susceptible to Lorentz force detuning because they have relatively large, flat sides that are flexible compared to very high β cavities.

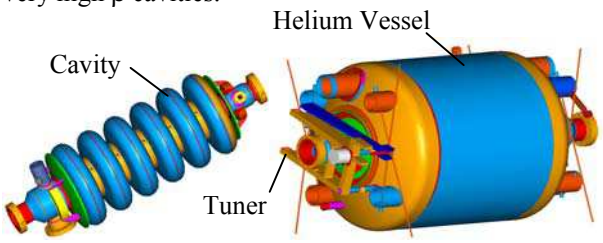

Figure 2: β=.61 cavity and helium vessel assembly.

3 COMPUTATIONAL TOOLS

SUPERFISH is used to compute the radiation pressures for each mesh element [2]. The finite element code, ABAQUS, computes the displacements for each mesh element [3]. The displacements are input back into SUPERFISH where the frequency of the deformed shape is calculated. For the dynamic calculations, the time varying radiation pressures are input into the ABAQUS model and the cavity displacements are calculated as a function of time. To calculate the frequency shift, select deformations are input into SUPERFISH.

The ABAQUS axisymmetric shell finite element model has one beam tube fixed and the other restrained by a spring (see Fig. 3). The spring is used to simulate the stiffness of the boundary condition. For example, the spring stiffness would correspond to the equivalent stiffness of the helium vessel and tuner in series when modeling the SNS assembly Lorentz force detuning.

The calculations for the niobium cavity assumed an elastic modulus of 16.4×10^6 psi (4K), a density of 0.313 lb/in^3, and a Poisson's ratio of .38.

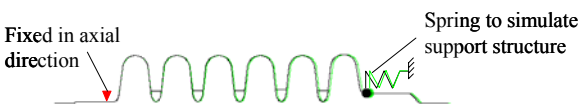

Figure 3: Axisymmetric ABAQUS finite element mesh.

4 STATIC LORENTZ DETUNING

4.1 VTA Testing

Three static Lorentz force detuning tests of the medium β cavity have been performed in the Vertical Test Area (VTA) at Jefferson Lab (see Fig. 4). The first test utilized a titanium fixture that had a calculated stiffness of 3.04×10^4 lb/in (5.33×10^6 N/m) to restrain the cavity. The cavity was then welded inside the prototype helium vessel and tested without a tuner. The only feature restraining the cavity was the relatively soft helium vessel bellows with a measured stiffness of 1.4×10^3 lb/in (2.45×10^5 N/m). Then a mock tuner was mounted between the helium vessel and cavity, increasing the assembly stiffness to a calculated 5.43×10^4 lb/in (9.51×10^6 N/m).

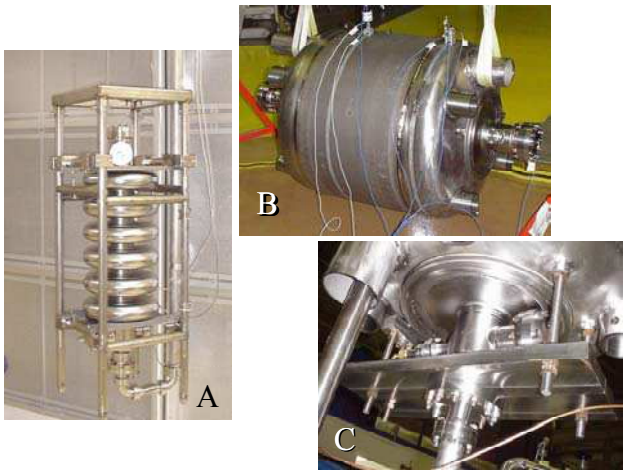

Figure 4: Cavity constrained by A. Ti fixture, B. helium vessel bellows, C. prototype helium vessel and mock stainless steel tuner.

4.2 Model Validation

ABAQUS finite element models calculated the deformations for the three stiffness values discussed above. The models showed very good agreement to the test data (see Table 1) especially when considering that calculations were used to estimate the restraint stiffness (except for the bellows) in addition to the Lorentz force detuning calculations. All calculations were within 17% of the test data. In addition, the high β=.81 cavity was tested in the titanium fixture, and compared extremely well to the calculation.

In addition to the test cases, completely fixed and free boundary conditions were analyzed to predict the extreme Lorentz force detuning values. The predicted SNS assembly stiffness of 1.1×10^5 lb/in (1.9×10^7 N/m) was simulated and produced a K_L of -3.6, exceeding the requirement of -3 Hz/(MV/m)^2. These calculations demonstrate the importance of the boundary conditions in determining the static Lorentz force detuning (see Fig. 5). In general, static Lorentz force detuning decreases with increasing boundary stiffness.

Table 1: Static Lorentz Detuning Comparison

	Test K_L [Hz/(MV/m)^2]	**Analysis** K_L [Hz/(MV/m)^2]
Free	--	-24.4
Helium Vessel Bellows	-18.0	-21.0
Titanium Test Fixture (β=.61)	-8.3	-7.0
Prototype He Vessel & Mock Tuner	-5.6	-5.3
SNS Assembly	--	-3.6
Fixed	--	-2.1
Titanium Test Fixture (β=.81)	-3.5	-3.5

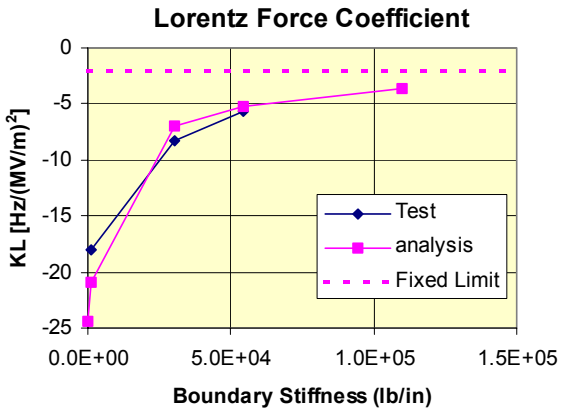

Figure 5: Lorentz force coefficient comparison as a function of boundary stiffness for the medium β cavity.

5 DYNAMIC LORENTZ DETUNING

5.1 SNS RF Pulse

The SNS RF pulse [4] has a 1ms flat-top (see Fig. 6) and is cycled at 60 Hz. Because the pulse contains a large amount of energy at a relatively high frequency (see Fig. 7), it is capable of exciting relatively high mechanical natural frequencies, certainly in the 480 Hz neighborhood.

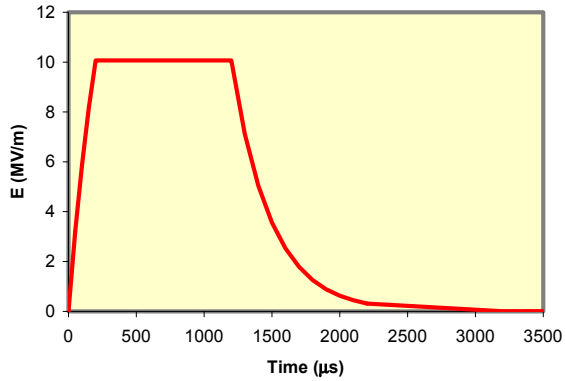

Figure 6: SNS RF pulse profile.

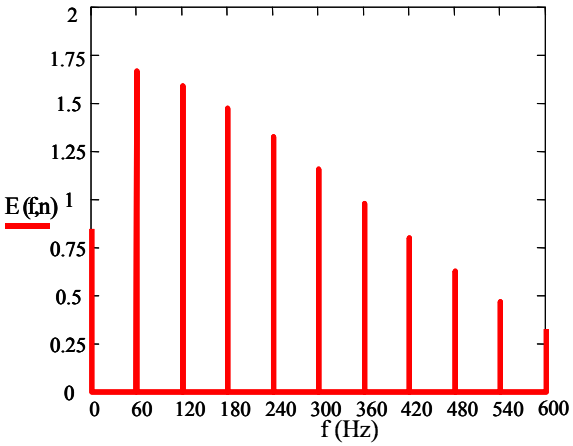

Figure 7: SNS pulse spectrum.

5.2 Boundary Stiffness

Three different stiffness values were used for the dynamic Lorentz force detuning calculations:

(1) The stiffness of 0.5×10^5 lb/in (0.9×10^7 N/m) corresponds to the calculated prototype helium vessel and mock tuner assembly stiffness.

(2) The stiffness of 1.1×10^5 lb/in (1.9×10^7 N/m) corresponds to the estimated SNS assembly stiffness. This stiffness calculation is based on the most recent helium vessel with stiffening features and the estimated tuner stiffness based on a TESLA tuner stiffness measurement.

(3) The stiffness of 1.9×10^5 lb/in (3.3×10^7 N/m) corresponds to the idealized SNS assembly stiffness and represents an upper limit value. This stiffness calculation is based on the most recent helium vessel with stiffening features and an estimated tuner stiffness based on stiffness calculations of the tuner components, not the assembly.

5.3 Calculated Axial Modes

The axial mechanical natural frequencies were determined for the three boundary stiffness values by performing an ABAQUS modal analysis. The first six mode shapes are shown in Figure 8 and the corresponding natural frequencies are shown in Table 2. The cavity has many modes between 60 and 480 Hz making the cavity susceptible to dynamic excitation. It is interesting to note that Mode 2 for the stiffness of 1.1×10^5 lb/in occurs at a calculated frequency of 182 Hz, very close to the 180 Hz harmonic. In addition, Mode 4 for the stiffness of 1.9×10^5 lb/in occurs at 365 Hz, very close to the 360 Hz harmonic. In fact, any stiffness between 1.9×10^5 and 1.1×10^5 lb/in will have a mode near a harmonic frequency. The modes for the stiffness of 0.5×10^5 lb/in are at least 9 Hz away from a harmonic frequency.

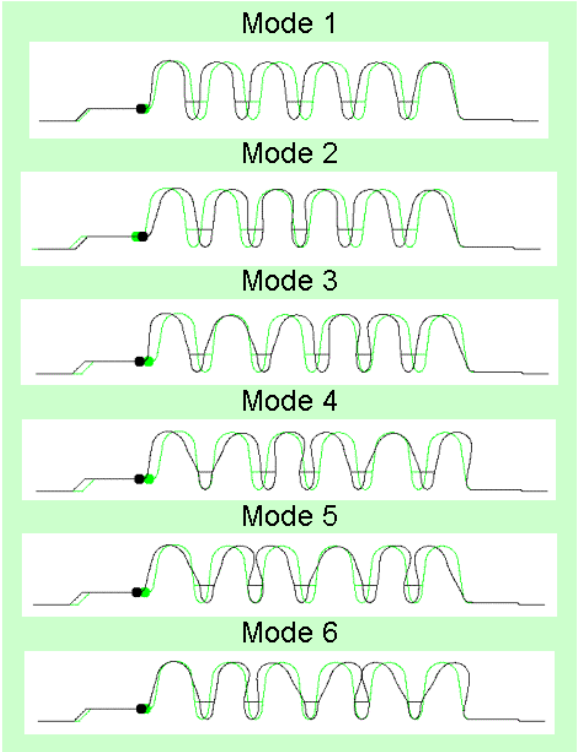

Figure 8: Modes shapes for the β=.61 cavity.

Table 2: Calculated Axial Modes

	Natural Frequency (Hz)		
Mode	**k=1.9x10^5 lb/in (3.3x10^{7}N/m)**	**k=1.1x10^5 lb/in (1.9x10^{7}N/m)**	**k=0.5x10^5 lb/in (0.9x10^{7}N/m)**
1	96	92	86
2	190	**182**	171
3	280	268	256
4	**365**	351	343
5	442	432	429
6	505	502	504

5.4 Cavity Response as a Function of Boundary Stiffness

A dynamic analysis, using ABAQUS, was performed to determine the time varying cavity response as a function of the boundary stiffness for the first two seconds of pulsed operation. These calculations assumed a 0.3% damping, and a 60 Hz pulse. Figures 9-11 plot the beam tube displacement as a function of time, not Lorentz force detuning. To calculate the Lorentz force detuning, cavity deformations were input into SUPERFISH at specific points in time. Although the time history plots are beam tube displacement and not frequency shift, they still provide an indication of the relative frequency shift amplitude.

Figure 10 plots the displacement for the initial 0.05 seconds and shows that the displacement of the cavity to the first pulse is inversely proportional to the boundary

stiffness. This is similar to the trend that was found for the static solution. However, the displacements increase with time for the stiffness values of $1.9x10^5$ and $1.1x10^5$ lb/in, while the $0.5x10^5$ lb/in case remains relatively constant with time. Closer examination at the end of two seconds (see Fig. 11) shows a very periodic response corresponding to approximately 360 Hz for the boundary stiffness of $1.9x10^5$ lb/in. A similar trend is shown for a stiffness of $1.1x10^5$ lb/in, except that the periodic response occurs at approximately 180 Hz. A comparison of the excited mode shape and the actual dynamic cavity shape after approximately two seconds (Fig. 12) provide more evidence that a natural frequency is being excited. The softest boundary condition ($k=0.5x10^5$ lb/in) shows a non-periodic response at 2 seconds indicating a mixed mode response.

The calculated maximum dynamic and static Lorentz force coefficients are shown in Table 3. The boundary stiffness values that produce a mode at one of the forcing harmonic frequencies produce a dynamic K_L two to three times the static value. For the case that didn't excite a single mode, the dynamic K_L is a factor of two below the static value.

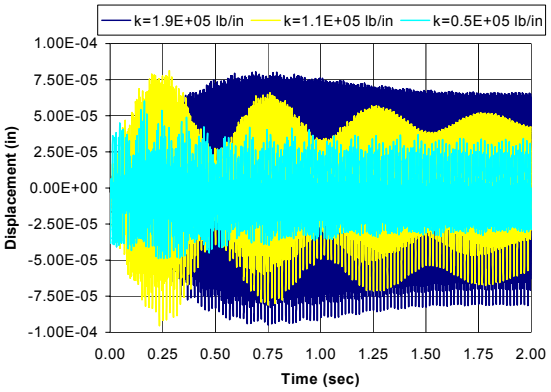

Figure 9: Comparison of cavity response with varied boundary stiffness.

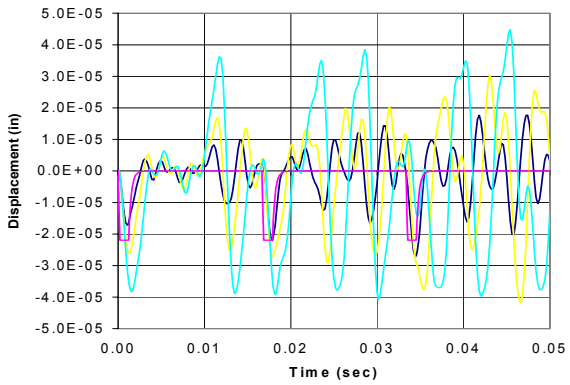

Figure 10: Comparison of cavity response with varied boundary stiffness at t=0 – 0.05 s.

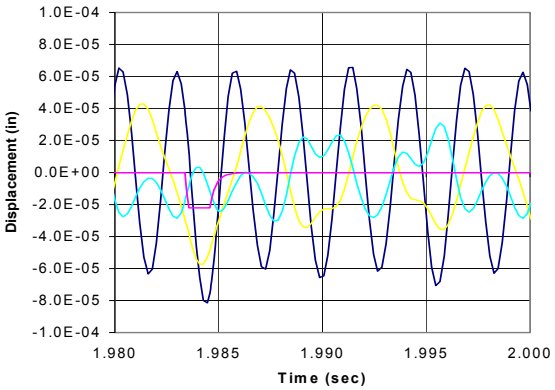

Figure 11: Comparison of cavity response with varied boundary stiffness at t=1.98 – 2 s.

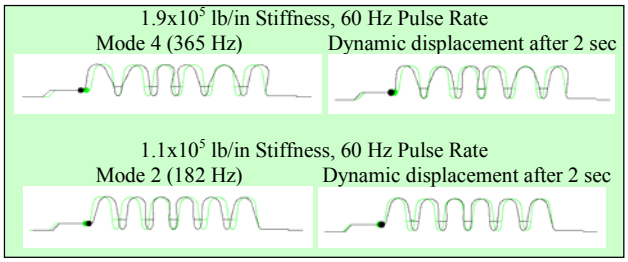

Figure 12: Comparison of mode shapes and dynamic displacement plots.

Table 3: K_L as a Function of Boundary Stiffness

Stiffness [lb/in]	**Dynamic K_L** [Hz/(MV/m)^2]	**Static K_L** [Hz/(MV/m)^2]
$1.9x10^5$	-8.6	-2.9
$1.1x10^5$	-8.9	-3.6
$0.5x10^5$	-2.4	-5.3

5.5 Cavity Response as a Function of Mechanical Damping

Dynamic analyses were performed on the medium β cavity with a boundary stiffness of $1.9x10^5$ lb/in and a pulse frequency of 60 Hz to determine the effect of damping. Tests to determine the damping have been completed for the cavity assembled into a prototype helium vessel and restrained by the mock tuner at room and liquid helium temperatures. The room temperature test suspended the helium vessel assembly from nylon straps. An accelerometer was mounted to one beam tube while a modal impact hammer struck the opposing beam tube. The liquid helium temperature test occurred while the helium vessel assembly was suspended in the VTA. A modal impact hammer struck the dewar lid while the cavity frequency shift was measured. The amount of damping in the ABAQUS model was adjusted until it produced a similar damping response for a single RF pulse input (see Fig. 13). The damping was determined to be approximately .3%. Analyses were also performed for .06 and .6% damping to bound the problem.

As expected, increasing the amount of damping decreases the maximum displacement (see Fig. 14) and as a result decreases the Lorentz detuning. The maximum Lorentz force detuning coefficients are shown in Table 4.

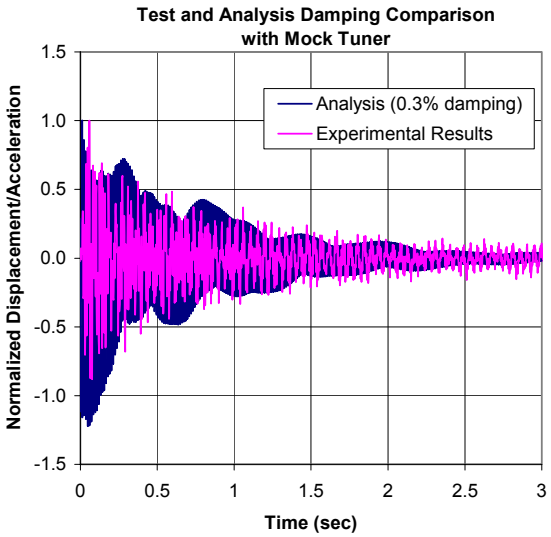

Figure 13: Test and analysis damping comparison with mock tuner.

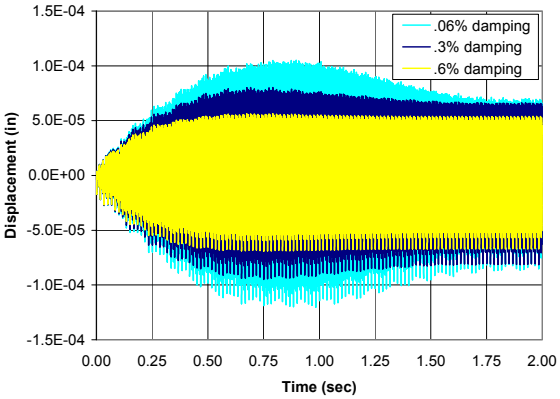

Figure 14 : Comparison of cavity response with varied damping ratios.

Table 4: K_L as a Function of Damping

Damping [%]	**Dynamic K_L** [Hz/(MV/m)^2]	**Static K_L** [Hz/(MV/m)^2]
.06 (Q=830)	-10.5	-2.9
.3 (Q=170)	-8.6	
.6 (Q=83)	-6.1	

5.6 Cavity Response as a Function of Pulse Frequency

Analyses were performed for a medium β cavity with a boundary stiffness of 1.9x10^5 lb/in and .3% damping, subjected to pulse frequencies of 60, 30, 10 and 59 Hz (see Fig. 15). The 60, 30, and 10 Hz pulse frequencies excite the 360 Hz cavity natural frequency, but the 10 Hz displacements are significantly lower than the 60 or 30 Hz pulse rate (see Fig. 16). The displacement amplitude may decrease with decreasing pulse rate because the 360 Hz mode is the 6th harmonic for the 60 Hz pulse, but is the 36th harmonic for the 10 Hz pulse and therefore less energy is available to excite the cavity at the lower pulse rate. The 59 Hz pulse rate also decreased the displacements and did not excite a particular mode. Its 6th harmonic was moved from 360 Hz down to 354 Hz, away from the cavity's natural frequency of 365 Hz. Table 5 shows the maximum Lorentz detuning coefficients as a function of pulse frequency.

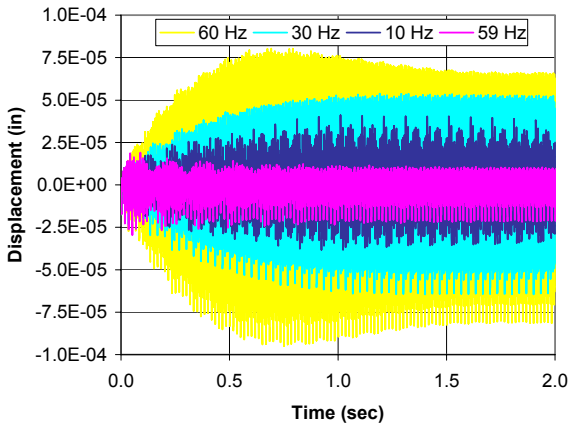

Figure 15: Comparison of cavity response with varied pulse frequencies.

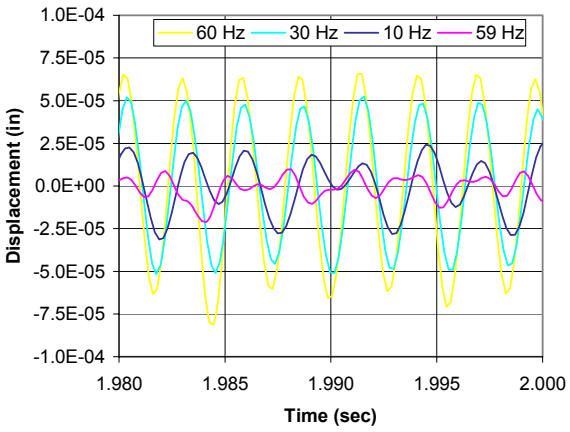

Figure 16: Comparison of cavity response with varied pulse frequencies at t=1.98-2s.

Table 5: K_L as a Function of Pulse Frequency

Pulse Frequency [Hz]	**Dynamic K_L** [Hz/(MV/m)^2]	**Static K_L** [Hz/(MV/m)^2]
60	-8.6	-2.9
30	-8.2	
10	-3.9	
59	-3.9	

5.7 Cavity Response as a Function of Pulse Width

Three RF pulses, having pulse flat-tops of .8, 1.5 and 2 milliseconds, were analyzed for a boundary stiffness value of 1.9×10^5 lb/in and .3% damping. The boundary stiffness analyzed causes the 360 Hz mode to be excited. The RF pulse spectrum for the three pulses (see Fig. 17) indicates that at 360 Hz, the .8 and 2 millisecond pulses have approximately the same energy while the 1.5 millisecond pulse has the most energy. The cavity response for the three pulses shows the same trend (see Fig. 18). The .8 and 2 millisecond pulses produce similar displacements while the 1.5 millisecond pulse produces the most displacement.

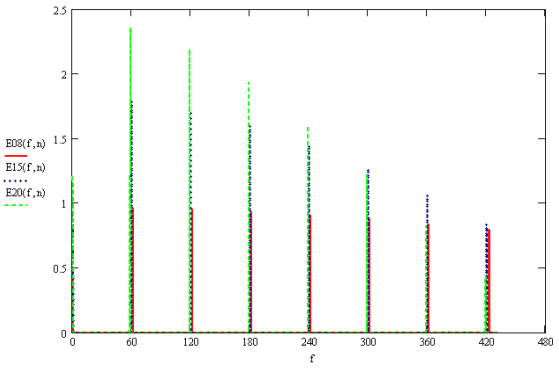

Figure 17: Comparison of spectrums for square pulses with widths of .8, 1.5 and 2 msec.

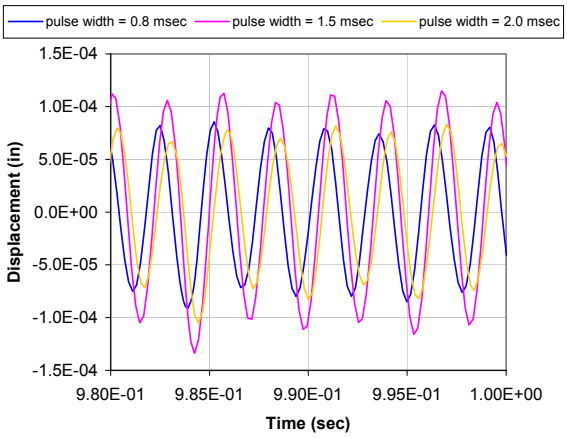

Figure 18: Comparison of cavity response with varied pulse widths.

5.8 Cavity Response as a Function of Stiffener Ring Position

Two additional analyses were performed for a stiffening ring at 100 mm and for stiffening rings at both 80 and 100 mm (see Fig. 19). Both of these cases move the cavity natural frequencies away from the forcing harmonics (see Table 6). The dynamic analyses were calculated for a boundary stiffness of 1.1×10^5 lb/in, a pulse rate of 60 Hz, and .3% damping. The displacement history shows that the 100 mm and the 80 plus 100 mm cases have significantly less displacement than the 80 mm ring case (see Figs. 20 & 21). The maximum Lorentz force detuning coefficients for the three cases are shown in Table 7. Notice that the double ring case develops similar displacements as the 100 mm case, but the Lorentz force detuning is significantly less. This is most likely the result of the two rings effectively stiffening the cavity wall between the two rings, limiting the detuning.

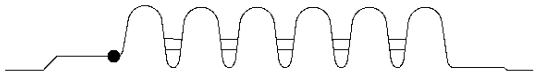

Figure 19: Axisymmetric finite element model of the .61β cavity with an additional 100mm stiffener ring.

Table 6: Calculated Axial Modes for Different Stiffener Ring Positions

	Natural Frequency (Hz)		
Mode	**100mm Ring**	**80+100mm Ring**	**80mm Ring**
1	103	102	92
2	212	212	182
3	325	329	268
4	439	446	351
5	551	557	432
6	658	664	502

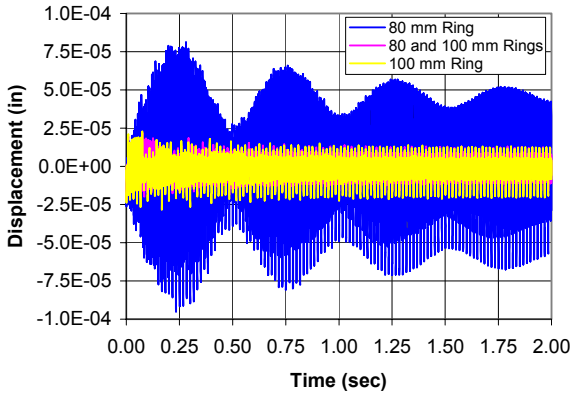

Figure 20: Comparison of cavity response with varied stiffener rings.

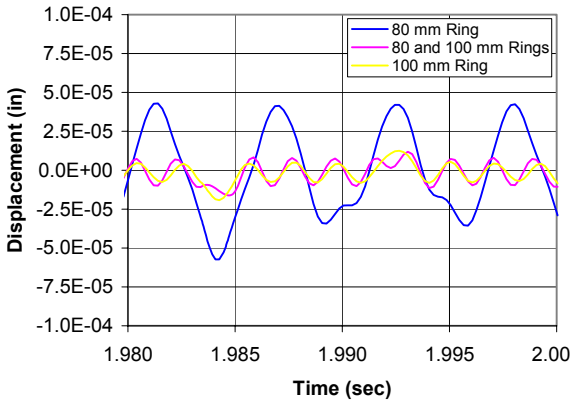

Figure 21: Comparison of cavity response with varied stiffener rings at t=1.98-2s.

Table 7: K_L as a Function of Stiffening Ring Position

Ring Location [mm]	**Dynamic K_L** [Hz/(MV/m)^2]	**Static K_L** [Hz/(MV/m)^2]
80	-8.9	-3.6
100	-3.8	-3.6
80 & 100	-2.0	-2.3

6 CONCLUSION

The modeling approach gives good agreement with the experimental results for the static Lorentz force detuning, and results indicate that the static SNS requirement will likely be exceeded for the current design. In general, increasing the boundary stiffness will decrease the static Lorentz force detuning.

Contrary to the static Lorentz force detuning behavior, increasing the boundary stiffness does not necessarily decrease the dynamic Lorentz force detuning. These analyses show that it is more important to avoid hitting a cavity natural frequency. In addition, only the dynamic Lorentz force detuning is important for a pulsed system, not the static Lorentz force detuning.

These calculations indicate that the medium β cavities are susceptible to dynamic Lorentz force detuning due to the high 60 Hz pulse rate and the many natural frequencies below 480 Hz. In order to determine if the analysis predictions are correct, dynamic Lorentz force detuning experiments need to be performed and compared to the results. Once the model is validated, recommendations to reduce the dynamic Lorentz force detuning can be made. These calculations also need to be performed on the β=.81 cavity.

7 REFERENCES

[1] Gigi Ciovati et al., "Lorentz Force Detuning for the SNS Cavities", presentation for LLRF Workshop, April 25-27, 2001.

[2] ABAQUS, Version 6.2.1. Hibbitt, Karlsson & Sorenson, Inc., 2001.

[3] James H. Billen & Lloyd M. Young, SUPERFISH, Version 6, Los Alamos National Laboratory, Los Alamos, NM.

[4] Ron Sundelin, Jefferson Lab, Newport News, VA.